Calcium Sorbent for the Enhanced Gasification & Pyrolysis of Biomass

UNDERGRADUATE THESIS

Presented in Partial Fulfillment of the Requirements for the Honors B.S. in Chemical & Biomolecular Engineering with Research Distinction

By

Nicholas Blum

Undergraduate Program in Chemical & Biomolecular Engineering

The Ohio State University

Committee:

Distinguished Professor, L.S. Fan, Advisor

Assistant Professor, N. Brunelli

Defended: 31st of March, 2014

Submitted: 11th of April, 2014

X

L.S. Fan
Distinguished Professor

ABSTRACT

With energy usage increasing steadily, many countries are looking to find new sources of energy to fuel the increased demand. One area of interest is the conversion of waste to fuel, one area of which is biomass. Biomass is waste biological product that serves no purpose and is typically discarded as waste, like sawdust generated by lumberyards, cornstalks from farms, etc. Biomass is abundant, but is not energy dense and generally requires a great deal of pretreatment before it can be used. Thus, it would be advantageous to derive and economical process to generate readily usable fuels, or even fuel bases, from this biomass. However, without employing catalysts or catalytic methods, it is difficult to break down biomass, due to its complex polymeric composition.

Calcium looping is a chemical looping process which utilizes calcium oxide (CaO) to capture carbon dioxide (CO2) and other pollutants from flue gas. While CaO has typically been used as a capture agent, it also has documented catalytic properties. CaO is a relatively abundant and inexpensive, and while it typically deactivates during carbon capture processes, its tar-cracking properties may prove to be effective in breaking down the complex ligno-cellulosic material for the generation of fuels. Additionally, it is possible that the CaO may retain its activity as a catalyst during proper regeneration.

This thesis investigated the operational parameters associated with the conversion of biomass to gaseous and bio-oil in the presence of a calcium sorbent. The kinetic and thermodynamic properties of the decomposition of biomass in the presence of calcium sorbent were explored; a model was constructed for the effect of CaO concentration on the pyrolysis and gasification of biomass; calcium hydroxide ($Ca(OH)_2$) was investigated as the source of steam (the oxidizing agent); a model for the production of bio-oil was proposed. Additionally, unexpected increased evolution of carbonaceous gases were observed at high loadings of CaO. Possible explanations were developed, and future work was suggested.

ACKNOWLEDGEMENTS

I would like to thank Dr. Fan for the opportunity to work in his lab, as well as Niranjani Deshpande for her continued mentorship and guidance. I thank the URO as well as the College of Engineering Research Scholarship in helping to fund this research. I would also like to thank my colleagues and friends within Chemical Engineering for their help and support.

TABLE OF CONTENTS

LIST OF FIGURES

LIST OF TABLES

I. INTRODUCTION, BACKGROUND, & SIGNIFICANCE

Biomass is a form of waste that results as a by-product of many industrial-agricultural operations. A few examples include sawdust from lumber mills, corn stalks from farms, paper pulp from paper factories, etc. This waste is generated on a relatively large scale, and, currently, is discarded mainly as simply trash from these processes. It would be advantageous to be able to recover some of the energy stared in this waste biological product that otherwise is not generally utilized.

In general, biomass is a poor fuel in and of itself for multiple reasons, first among which is its solid-state nature. Solids, in general, are much more difficult to process and transport than liquid or gaseous fuels. Second, biomass typically contains a large amount of water within its cell structure, greatly reducing the extractable energy one can obtain by burning biomass directly. Lastly, many of the chemical compounds present in biomass tend not to decompose or oxidize completely, and form poly-aromatics as a sort of non-reactive tar in the reactor system, again, decreasing the amount of energy that can be extracted. Refer to Equations 1, 2, and 3 for the overall reaction design concept.

$$biomass + \Delta \rightarrow tars + volatiles + char + gases \quad \text{(Equation 1)}$$

$$tars + CaO + \Delta \rightarrow volatiles + char \quad \text{(Equation 2)}$$

$$volatiles + char + O_2 + \Delta \rightarrow gases \quad \text{(Equation 3)}$$

The objective of this thesis study was to conduct proof-of-concept testing of the use of a calcium looping mechanism for the conversion of biomass into gaseous fuels during pyrolysis and gasification, where pyrolysis is the breakdown of a fuel under anaerobic conditions, and gasification is the partial oxidation of a fuel with an oxidizing agent such as air or steam to produce gases such as hydrogen (H_2) and methane (CH_4). The calcium looping system has traditionally been used as a carbon-capture technique to remove carbon dioxide (CO_2) from flue gas (Blamey, Anthony et al. 2010) (Florin and Harris 2008) (Ramkumar

and Fan 2010) (Ramkumar and Fan 2010). This primarily involves passing the flue gas through a CaO filled reactor, in which the reversible carbonation of CaO takes place shown in Equation 4.

$$CaO + CO_2 \leftrightarrow CaCO_3 \quad \text{(Equation 4)}$$

The calcium carbonate ($CaCO_3$) is then cycled to a separate reactor, a calciner, which heated the $CaCO_3$ to higher temperatures (>750℃) which caused the reaction in Equation 1 to occur in the reverse direction, evolving CO_2 into a pure stream for further treatment and possible sequestration (Blamey, Anthony et al. 2010). However, there was a significant issue with this industrial system in that the CaO would sinter at the calciner temperatures causing it to deactivate, which increases the required amount of CaO in the looping process causing a significant increase in capital and operating costs (Borgwardt 1989). Another looping mechanism was proposed by Fan et al. incorporated a hydration step to help slow the effects of deactivation in the CaO (Fan, Li et al. 2008). In this case, the flue gas was passed through a calcium hydroxide $Ca(OH)_2$ slurry to preferentially carbonate the $Ca(OH)_2$ to $CaCO_3$ through the reaction given in Equation 5 (Ramkumar and Fan 2010, Wang, Ramkumar et al. 2010).

$$Ca(OH)_2 + CO_2 \leftrightarrow CaCO_3 + H_2O \qquad \text{(Equation 5)}$$

This $CaCO_3$ was then calcined to evolve the captured CO_2 and hydrated to allow for better reactivation.

While the calcium looping mechanism has, to date, been used primary as a method of CO_2 capture, CaO actually exhibits substantial catalytic capabilities in terms of the breakdown of tars and other long-chain, poly-aromatics (Seshadri and Shamsi 1998) in additional to standard breakdown of coal tars. Biomass demonstrates low conversion when decomposed on its own, but CaO can help with the breakdown of the leftover tars to achieve greater conversion (Taralas, Vassilatos et al. 1991, García, Alarcón et al. 1999, Han and Kim 2008). By contacting the CaO or $Ca(OH)_2$ directly with the biomass, the conversion of the biomass could be increased through pyrolysis or gasification, respectively, as in the HyPrRing process (Lin, Suzuki et al. 2001). The looping mechanism would concurrently regenerate the CaO/$Ca(OH)_2$ for further catalytic breakdown of more biomass material.

This thesis investigates the operational parameters that should be optimized on a bench scale, so that an industrial process may be developed for the increased conversion and recovery of chemical energy from waste biomass using a chemical looping mechanism.

II. EXPERIMENTAL METHODOLOGY

In this section, the experimental methodology for the conducted tests is documented. The steps for calibration and each set of experiments are revealed, and the overall process is described. The procedure for the testing of the individual parameters is also described.

Hazard Identification & Safety

Throughout all experimentation, proper personal protective equipment (PPE) was worn and standard lab protocol was followed in order to maintain safety for the experimenters. As general lab practice, eye protection was worn whenever experiments were being conducted, as well as closed-toed shoes, long pants, and long-sleeved shirts. Proper handling of cylinder was maintained whenever they needed to be changed in order to minimize risk of accidents. All cylinders were fastened to a support system to prevent falling and potential fracturing of the cylinders.

All experiments were carried out in a room under negative pressure, in order to reduce exposure to any harmful gases (e.g. CO, CH_4) as well as any fine particulate matter that was kicked up in the process of preparing the samples. When excess particulate matter was anticipated, experimenters wore filtration masks in order to maintain respiratory health.

Sample Preparation

The biomass used during experimentation was a mixture obtained from softwood pines from the Midwestern and Southern United States. The dried wood was pressed into pellets and subsequently ground by a ball mill into a maximum of 500 micron pieces for the purposes of this study. This biomass was obtained from BMQ Inc. The ultimate analysis of the biomass can be found in Table 1.

Table 1: ultimate analysis of the biomass used in this study.

Wt.% (as received)	Wt.%, Dry Basis						
Residual Moisture	Ash	Carbon	Hydrogen	Nitrogen	Sulfur	Chlorine	Oxygen by difference
5.47	1.07	51.33	6.27	<0.1	0.12	0.0127	41.20

The CaO was prepared from a bulk $CaCO_3$-$Ca(OH)_2$ mixture by calcination in a furnace at 950℃ for typically 2 hours (but occasionally up to 9 hours if calcination occurred overnight). The calcined CaO was then cooled to 300℃ slowly as to maintain the temperature such that the hydration of the CaO did not occur to any appreciable extent. The CaO was then cooled rapidly from 300℃ to room temperature.

Analysis Methods

Thermogravimetric Analysis (TGA)

TGA were primarily carried out as a verification of the CaO purity throughout experimentation using a Perkin Elmer Pyris1. CaO, over time, will preferentially form $Ca(OH)_2$ and then $CaCO_3$ since those are its more stable thermodynamic states. CaO used for these experiments were tested via a temperature ramp of the TGA to 750 ℃ in order to devolve any remaining carbonate and hydrate, which allows for the calculation of the true composition of the CaO. A sample was considered to be sufficiently pure if the target compound's concentration was 75% or greater.

Gas Chromatography (GC)

Gas chromatography detects the presence and relative amounts of various gases. An Agilent CP-4900 micro-GC is the primary mode of analysis for the experiments. Gases enter the micro-GC at the sample port, and the time that it takes for the gases to elute through the columns are characteristic for each gas, allowing for identification of the gases. Further, the micro-GC plots the relative concentrations of each of

the gases as areas underneath the characteristic peak of each graph; this allows for the determination of the exit dry gas composition (minus steam) of the gases being evolved from the reactor. Using this information in conjunction with proper calibration, the absolute amounts of gases evolved relative to biomass can be determined.

JMP 9 & Statistical Analyses

JMP 9.0.0 from SAS is a statistical analysis software on which all statistical tests were performed. The alpha value for all statistical tests was 0.05. For ANOVA tests, the null model was simply the average of all of the points. Once a model passed the ANOVA test, the individual parameters of the model were tested to be statistically significant; if a parameter of the model was shown to be insignificant, it was removed from the model and the ANOVA test was conducted again on the revised model. All numerical factors were coded to provide consistency in the evaluation of our model. For plots of the models in JMP, the darker shaded region corresponds to a 95% confidence interval on the true model, and the lighter shaded region corresponds to a 95% confidence interval for the true mean of the response variable at a given independent variable.

Calibration

For the calibration of the micro-GC, multiple different gaseous mixtures were used for accurate determination of the quantity of the gases evolved from the reaction. Table 1 shows the five different gas mixtures used and their compositions.

Table 2: calibration gas mixtures.

Gas Component	Calibration Mixture 1 Composition (%)	Calibration Mixture 2 Composition (%)	Calibration Mixture 3 Composition (%)	Calibration Mixture 4 Composition (%)	Calibration Mixture 5 Composition (%)
Methane	-	-	-	20	20
Hydrogen	-	-	5	-	4
Nitrogen	90.5	97	95	72.3	76
Carbon Dioxide	-	3	-	-	-
Carbon Monoxide	9.5	-	-	7.7	-

Once the GC was calibrated, the flow rate was determined by an Agilent ADM2000 Universal Gas Flowmeter. For all experiments, the total flow rate into the reactor was kept constant at 200mL/min at standard conditions (1atm and room temperature).

General Setup & Methods

A schematic diagram of the overall experimental set-up can be found in Figure 1.

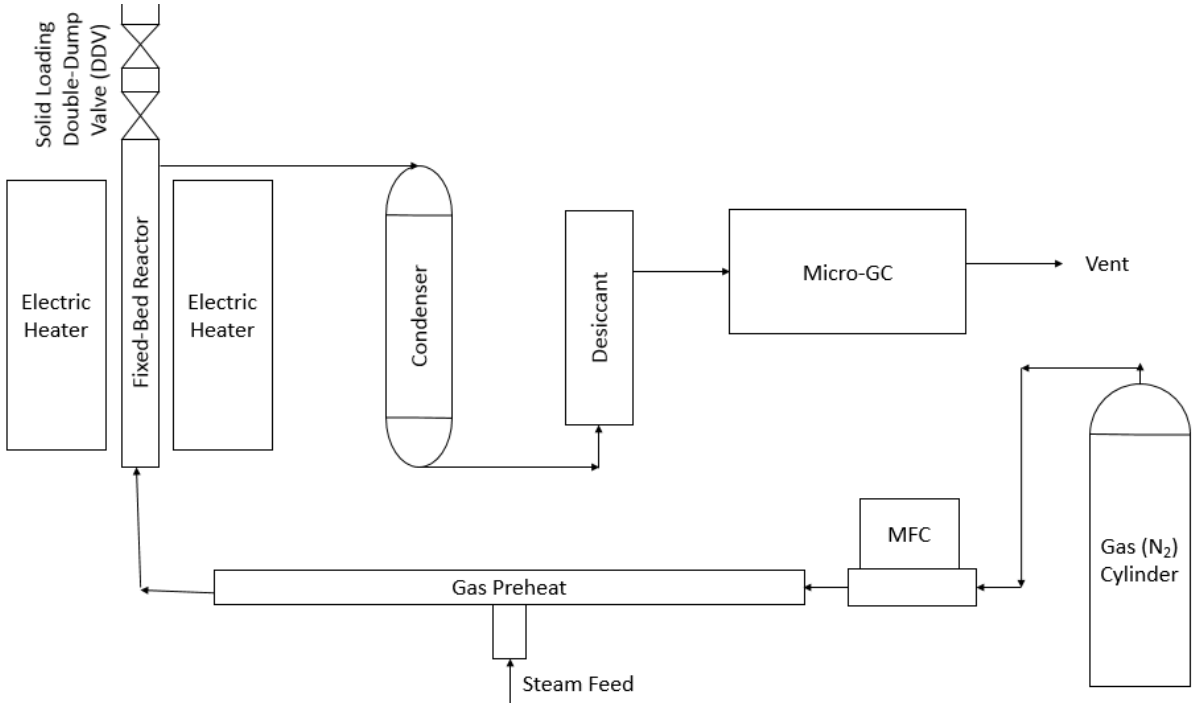

Figure 1: a schematic diagram of the experimental setup with legend.

Gas cylinders were fed into a mass flow controller (MFC) which then fed into the system. The gases were firs preheated in a heat exchanger using electrical heating tape; the gas was then fed directly to the bottom of a fixed bed reactor which was located within an electrically heated furnace (or reactor). After exiting the reactor through the top, the reactor effluent was then sent to another heat exchanger, the condenser, which utilized water at 4℃ where water and any remaining bio-oil is condensed out. The water was pumped using a Model 100DM ISCO Syringe Pump. The gases then passed through a desiccant bed of Drierite, which adsorbed any remaining water; the dry gas mixture then passed to the GC where samples were taken and analyzed. Only nitrogen was fed to the reactor during all experiments (with the exception of steam during gasification). GC samples were compiled into a report for analysis, and all reactor contents were weighed post experiment in order provide a final sample weight after pyrolysis and/or gasification.

Optimization Testing, Slow Pyrolysis, & Gasification

For the optimization experiments, the reactor was pre-loaded with mixture of biomass and 25%[1] CaO as well as pure biomass as a control, and was conducted at multiple different steam flow rates and temperatures. A table of the performed experiments for the optimization tests can be found in Table 2.

Table 3: optimization experiment runs at 25 wt% CaO to biomass ratio; these were conducted in the addition of a control.

Temperature (℃)	Steam Concentration (%)
450	5
550	15
650	30

For each temperature specification, the biomass calcium oxide mixture was heated from room temperature to the experiment temperature by use of the electric heater and a Thermolyne temperature controller. The biomass was then pyrolyzed until the steady-state temperature was reached, at which point steam was fed

[1] For the purposes of this thesis, all weight fractions (wt%) will be expressed as the weight fraction relative to the weight of biomass loaded.

to the reactor at the specified flow rate in order to gasify the sample. The standard total volumetric flow rate through the reactor was held constant at 200mL/min (at 1atm and room temperature) during gasification, but the steam was only fed once the reactor reached steady state. The GC took samples throughout the temperature ramp/pyrolysis through the gasification for about an hour. Temperatures were recorded throughout the temperature ramp at every GC sample time.

Fast Pyrolysis Experiments

For the fast pyrolysis experiments, the pressure in the system was held constant via the pressure controller, and the temperature of the reactor was maintained by calibrating the external furnace thermocouple relative to the interior thermocouple which was removed to include a double-dump valve assembly on the top of the reactor. All fast pyrolysis experiments were held at an external measured temperature of 410 ℃ corresponding to an internal temperature of 550℃. The pressure was held at approximately 3psig. The experiments involved varying the amount of calcium sorbent relative to the biomass weight. The biomass weight was kept constant at approximately 3.15g. The tested concentrations can be found in Table 3.

Table 4: tested loading of CaO relative to the biomass weight.

CaO Loading (wt%)
0
10[2]
25
35[2]
50
100
200

The volumetric flow rate was held constant at 200mL/min at standard conditions. The reactor was heated for 0.5 hours until it reached steady state, at which point, the CaO/biomass mixture was fed into the reactor via the double-dump valve at the top of the furnace and the GC was simultaneously initialized to start taking

[2] Indicates that the experiment was run with a filter and without pressure control.

samples. At the end of fast pyrolysis experiments, the lines were drained and all recoverable bio-oil was collected and weighed.

Gasification Experiments

For the fast gasification experiment, the experimental methodology was similar to that of the pyrolysis experiments with a few exceptions. For all fast gasification experiments, the steam concentration in the feed was kept constant at 30% of the total gaseous flow rate into the reactor. Again, the total gas flow rate into the reactor was kept constant at 200mL/min at standard conditions; thus, the nitrogen flow rate was kept constant at 140mL/min. Gasification took place isothermally at 550℃ and at 3psig. Again, CaO concentration was varied relative to a constant biomass weight. Table 4 shows the run variations for the fast gasification experiments.

Table 5: various CaO concentrations explored for the fast gasification experiments.

CaO Concentration (wt%)
0
25
50
100

The sample was fed to the reactor one half hour after heating began, and 15 minutes after steam was started to be fed into the reactor. The GC simultaneously began taking samples at the time the sample was dropped into the reactor.

$Ca(OH)_2$ Oxidizing Experiment

For the $Ca(OH)_2$ experiment, $Ca(OH)_2$ was studied as a potential source for the oxidizing agent for the chemical looping mechanism. $Ca(OH)_2$ was loaded in a 50wt% relative to the biomass at the same reaction conditions as fast-gasification, only with the absence of steam being fed to the reactor via the water pump. GC sampling began simultaneously with the dumping of the $Ca(OH)_2$/biomass mixture into the reactor.

III. RESULTS, ANALYSES, & DISCUSSION

This section details the results of the experiments described in the previous section, along with associated statistical analysis and discussion.

Optimization Results

For the optimization of the operating conditions, it was desired to determine the temperatures at which gave ample levels of combustion as well as pyrolysis of the biomass mixture. The steam rate was varied to determine the effect of steam on the evolution of hydrogen. In general, CO_2 is the best indicator of the level of combustion occurring, however, for these experiments CaO was loaded in conjunction with the biomass. It was assumed that for all operating conditions, the amount of CO2 captured by a constant was approximately constant, since the level of CaO loading is constant throughout. Thus, we can make comparisons between operating conditions on the amount of CO_2 evolved with relation to the level of combustion. The graph of the evolution of CO_2 can be found in Figure 2 for a steam inlet of 5% by volume.

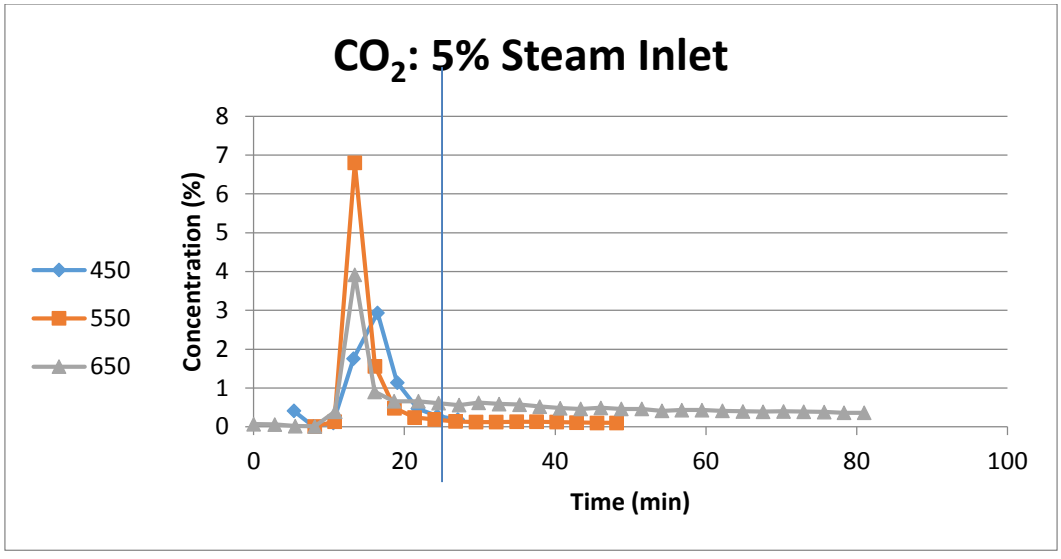

Figure 2: CO_2 concentration in the reactor exit gases plotted against time at a constant steam flow rate (5% volume fraction of total inlet gases) with varying temperature (℃); the blue line denotes the steam injection time.

This graph can be compared to the evolution of CO_2 at 15% and 30% in Figure 3 and Figure 4, respectively.

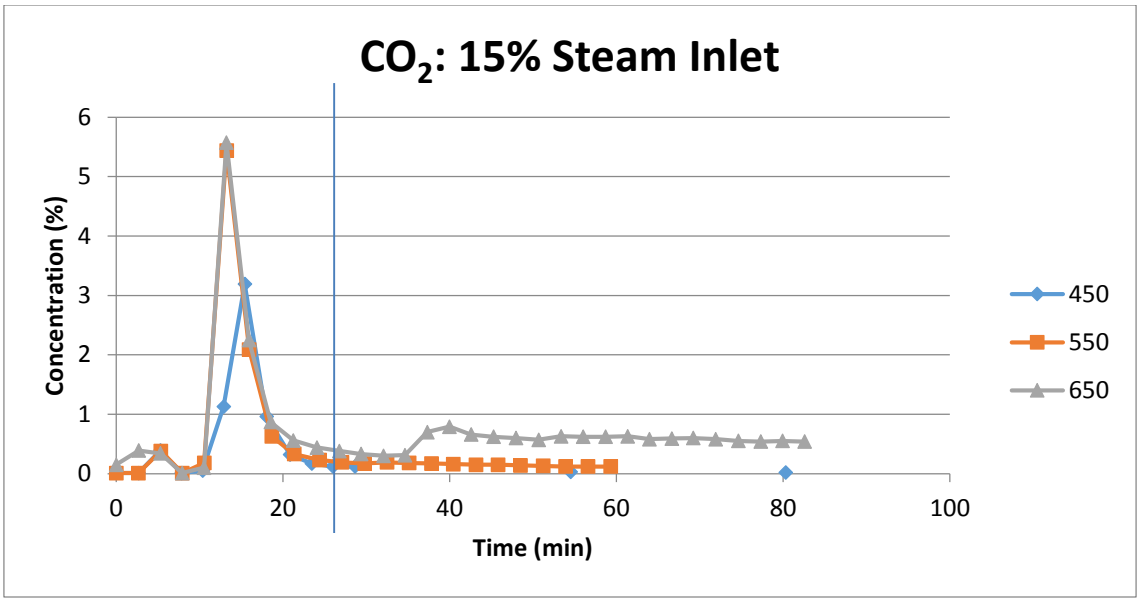

Figure 3: CO_2 concentration in the reactor exit gases plotted against time at a constant steam flow rate (15% volume fraction of total inlet gases) with varying temperature (℃the blue line denotes the steam injection time.

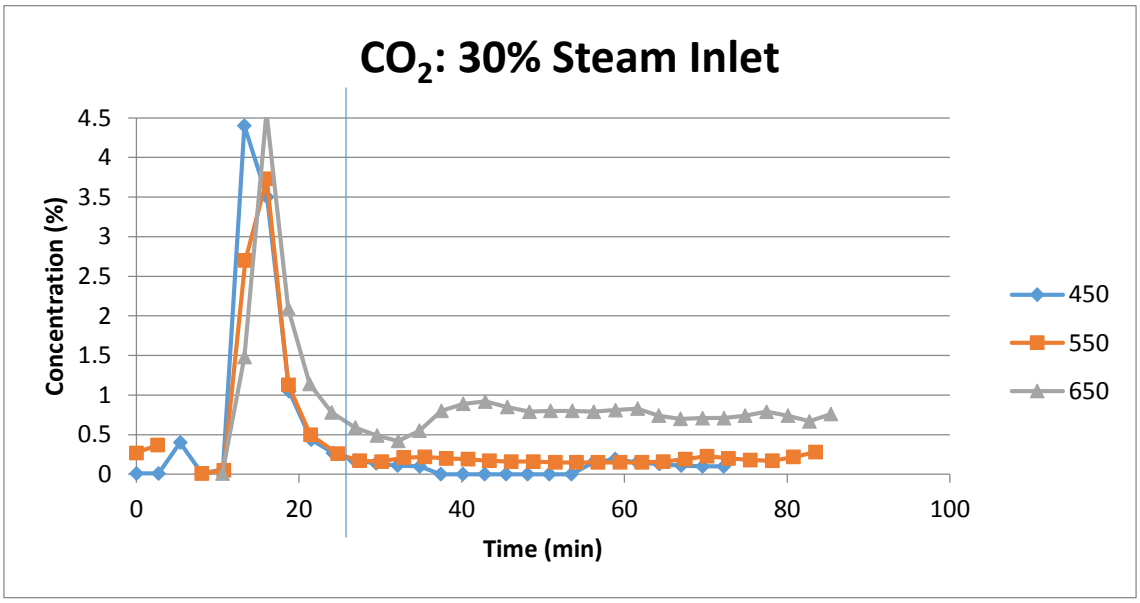

Figure 4: CO_2 concentration in the reactor exit gases plotted against time at a constant steam flow rate (30% volume fraction of total inlet gases) with varying temperature (℃); the blue line denotes the steam injection time.

From these graphs, we can see that 550℃ yields sufficient CO_2 during the pyrolysis of the biomass/CaO mixture. It can be observed that CO_2 evolution is greatest at 650℃ during gasification, however, for the study of the catalytic effects of the CaO on the gasification of biomass, we choose 550℃. This ensures that complete combustion of the biomass is not occurring and that catalytic effects of the CaO will be more

evident if they are present. Based upon our observations of the CO_2 concentrations, we would expect to see a corresponding increase in H_2 production from the oxidation of carbon by steam. These expectations are confirmed by examination of the evolution of H_2 at 5%, 15%, and 30% steam at varying temperatures in Figures 5, 6, and 7, respectively.

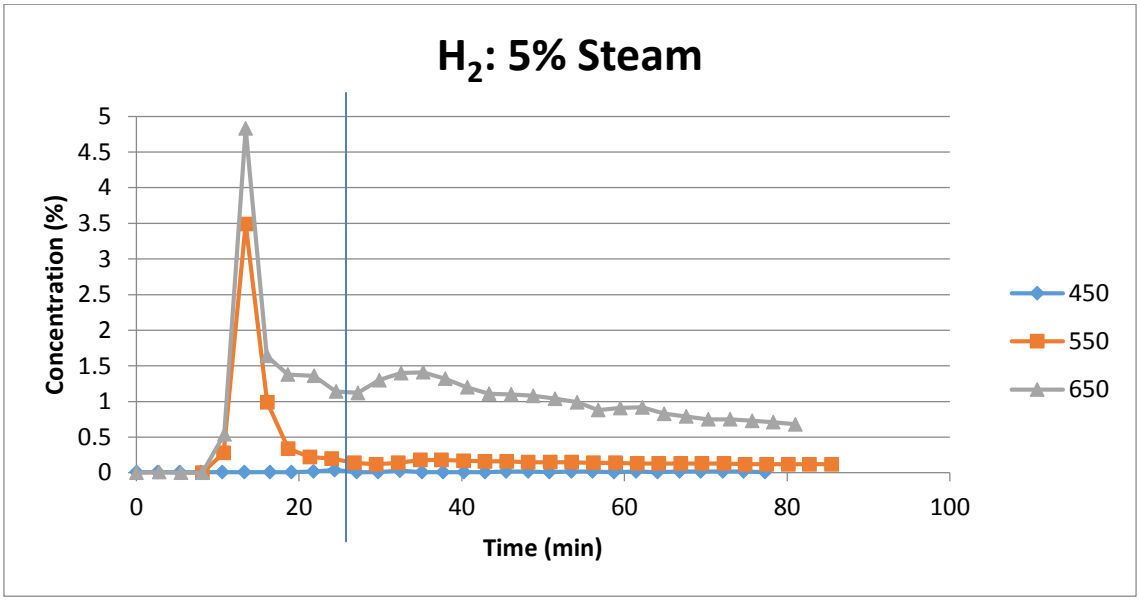

Figure 5: H_2 concentration in the reactor exit gases plotted against time at a constant steam flow rate (5% volume fraction of total inlet gases) with varying temperature (℃); the blue line denotes the steam injection time.

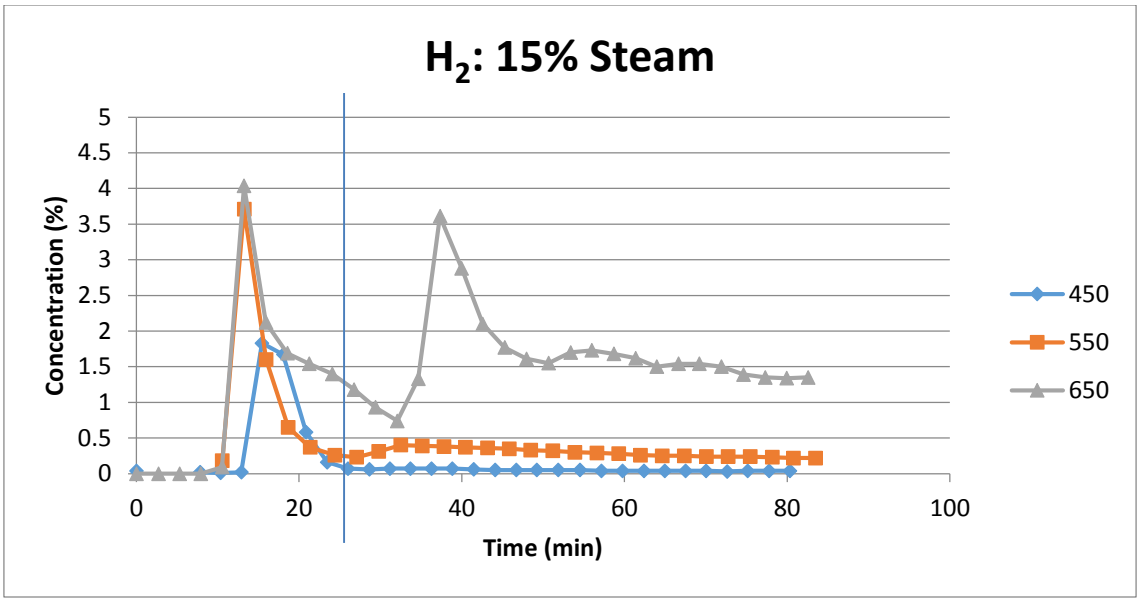

Figure 6: H_2 concentration in the reactor exit gases plotted against time at a constant steam flow rate (15% volume fraction of total inlet gases) with varying temperature (℃);; the blue line denotes the steam injection time.

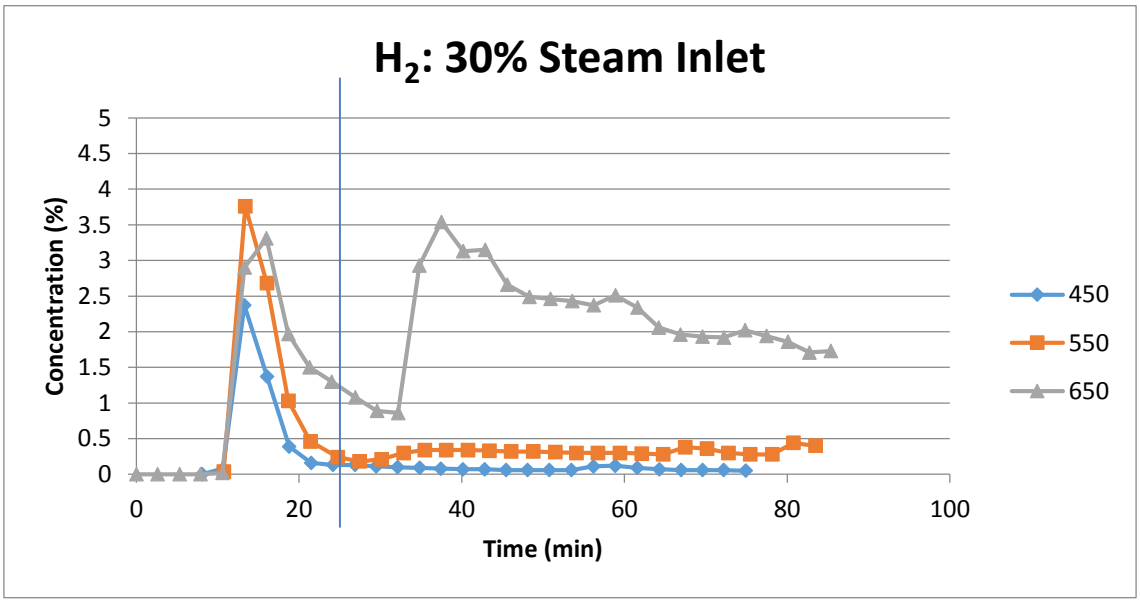

Figure 7: H_2 concentration in the reactor exit gases plotted against time at a constant steam flow rate (30% volume fraction of total inlet gases) with varying temperature (℃); the blue line denotes the steam injection time.

Again, it is clear that actual operating conditions for gasification would be at 650℃, the subject of interest is the catalytic effect of CaO, and thus we see again that the optimum temperature for studying these effects is 550℃. For the purposes of these experiments, CH_4 is assumed to be a sign of other light volatiles being evolved (e.g. ethane). Now, we want to look at CH_4 evolution to determine how our operating conditions

effect the generation of hydrocarbons and other light tars/volatiles at 5%, 15%, and 30% steam concentrations at varying temperatures in Figures 8, 9, and 10, respectively.

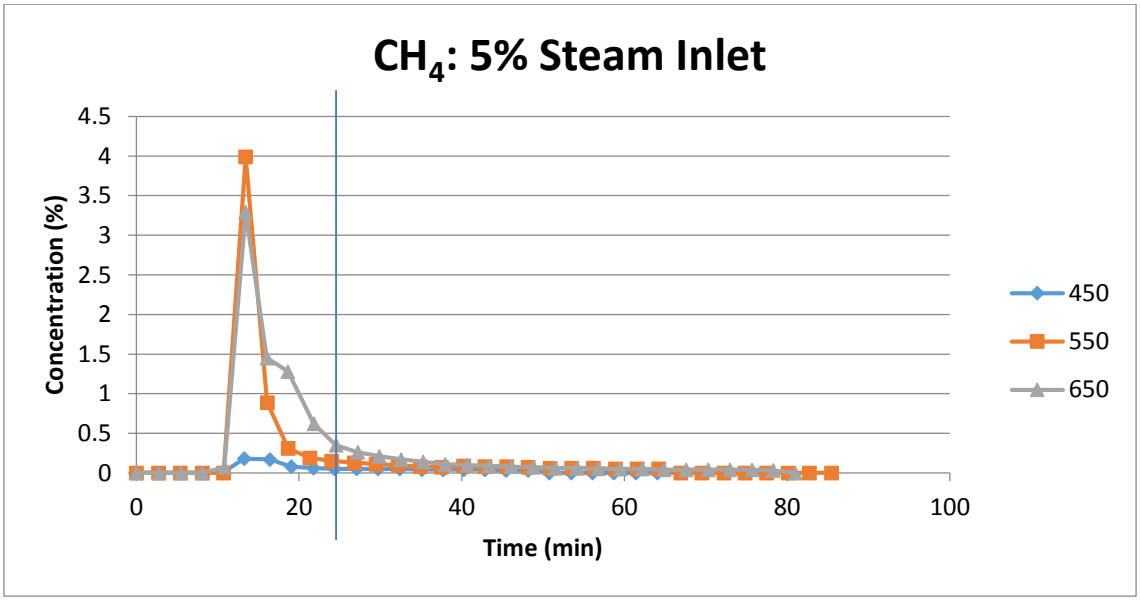

Figure 8: CH_4 concentration in the reactor exit gases plotted against time at a constant steam flow rate (5% volume fraction of total inlet gases) with varying temperature (°C); the blue line denotes the steam injection time.

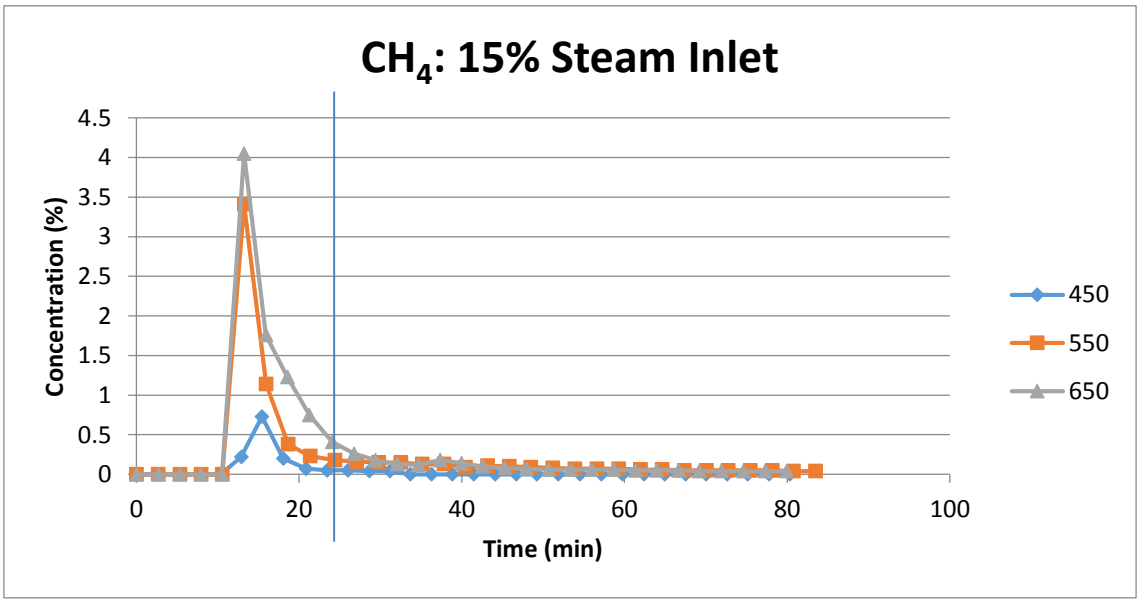

Figure 9: CH_4 concentration in the reactor exit gases plotted against time at a constant steam flow rate (15% volume fraction of total inlet gases) with varying temperature (°C); the blue line denotes the steam injection time.

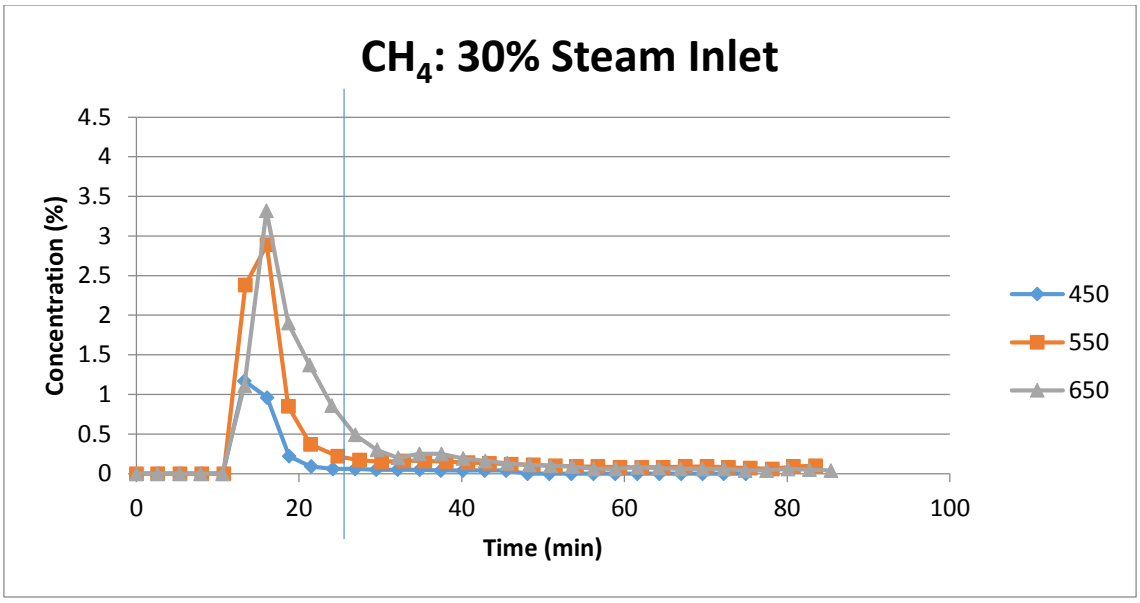

Figure 10: CH_4 concentration in the reactor exit gases plotted against time at a constant steam flow rate (30% volume fraction of total inlet gases) with varying temperature (℃); the blue line denotes the steam injection time.

Figures 8, 9, and 10 support the choice of 550℃ as sufficient CH_4 evolution can be observed even at that temperature. Thus, we can conclude that for the purposes of this experiment, sufficient devolatilization can be observed at 550℃. We can also look at CO evolution to support our conclusion at 5%, 15%, and 30% steam concentrations and varying temperatures in Figures 11, 12, and 13, respectively.

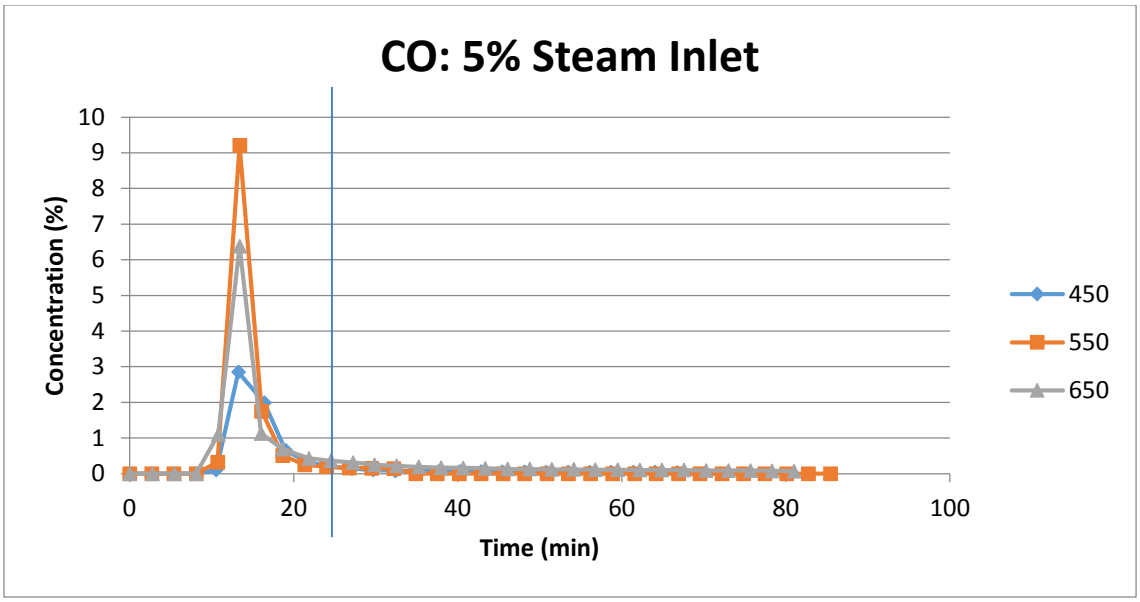

Figure 11: CO concentration in the reactor exit gases plotted against time at a constant steam flow rate (5% volume fraction of total inlet gases) with varying temperature (℃); the blue line denotes the steam injection time.

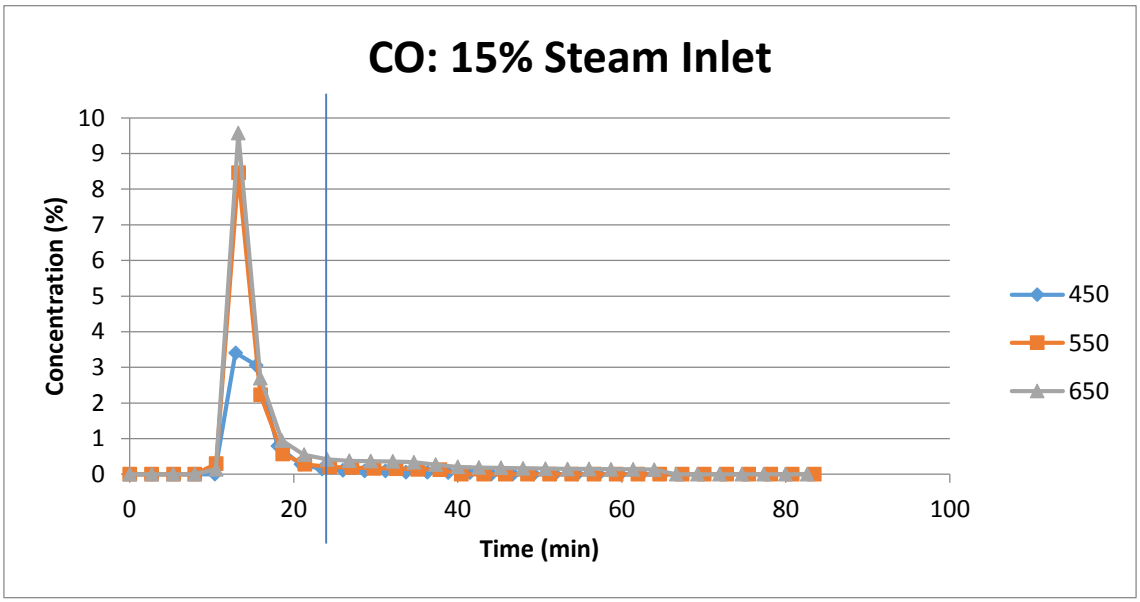

Figure 12: CO concentration in the reactor exit gases plotted against time at a constant steam flow rate (15% volume fraction of total inlet gases) with varying temperature (℃); the blue line denotes the steam injection time.

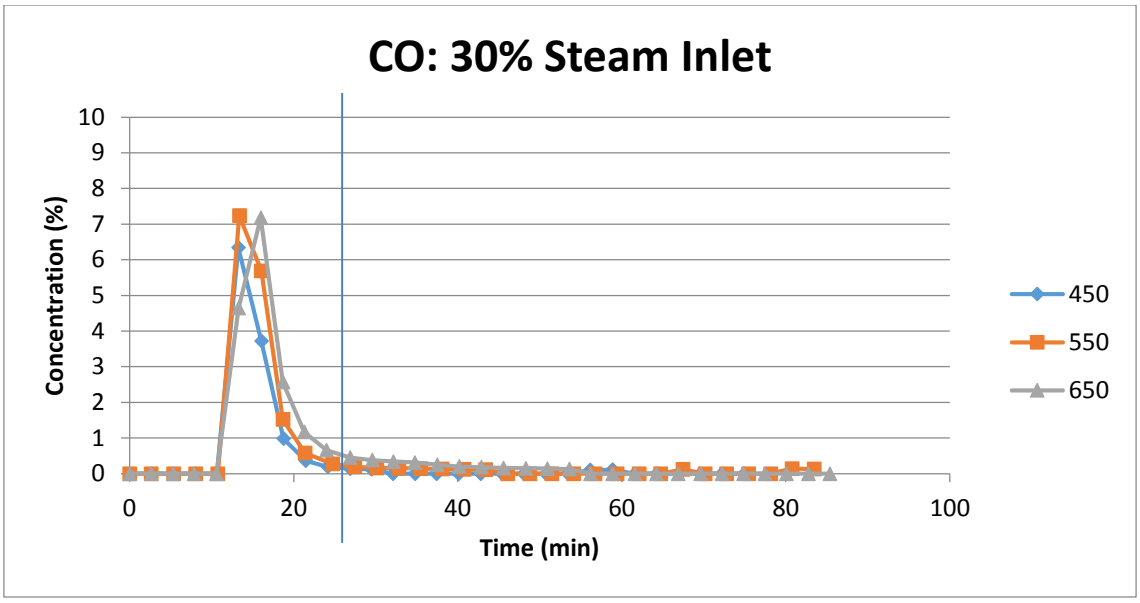

Figure 13: CO concentration in the reactor exit gases plotted against time at a constant steam flow rate (30% volume fraction of total inlet gases) with varying temperature (℃); the blue line denotes the steam injection time.

In terms of choosing a steam concentration for the inlet gas flow, a corresponding increase in the partial oxidation of the biomass can be seen with increasing steam concentration. This is to be expected, and 30% steam concentration was chosen since the limitation of the oxidizing agent was not a primary factor of interest during these experiments.

In conclusion, the temperature of 550℃ was chosen in order to best study the effects of CaO concentration on the decomposition of biomass during pyrolysis and gasification. Further, for gasification, a 30% steam concentration was chosen since this was the concentration that allowed for maximal conversion at any given temperatures and limiting the oxidizing agent is not a significant factor interest for the following experiments.

Fast Pyrolysis Results

For pyrolysis, Figure 14 shows the different types of conditions and their effects on the total gaseous evolution.

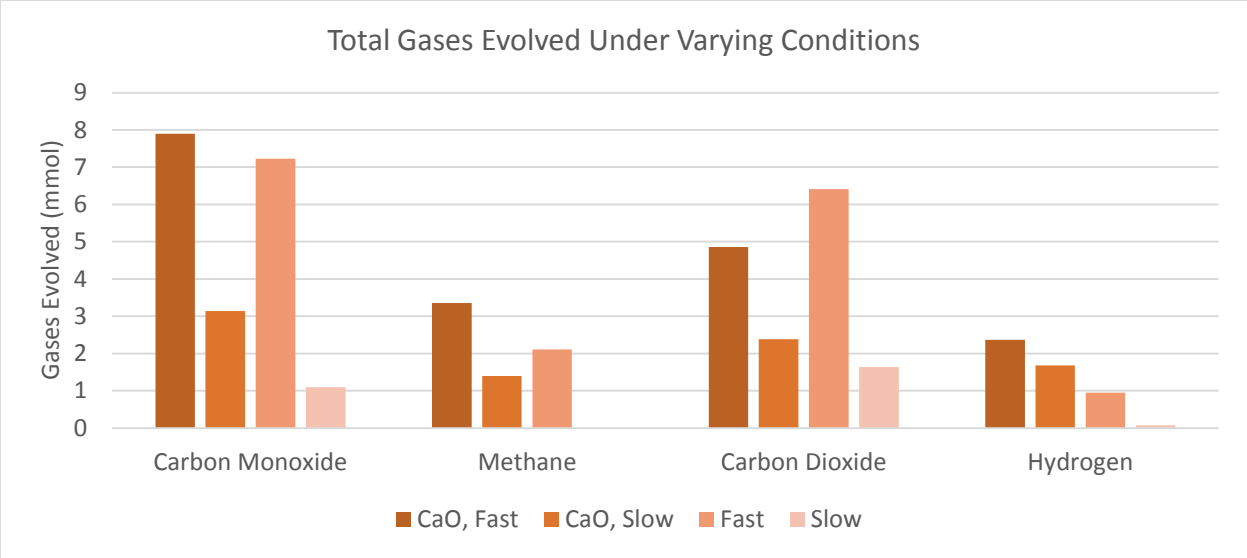

Figure 14: bar chart of the total amount of gases (CO, CH_4, CO_2, and H_2) evolved during pyrolysis (fast or slow) and whether or not CaO was present in a 25wt%. It is possible that there is no observed CH_4 for slow pyrolysis due to a merge with the CO peak in the micro-GC; however, it is likely not significant based on our findings.

From Figure 14, it is apparent that fast pyrolysis generates more gases overall, and, since the mass balances must remain constant, this corresponds to an increased breakdown in the biomass present. These results imply that the breakdown of the biomass is largely determined by kinetics, and that, as a general trend, faster pyrolysis and breakdown of the biomass corresponds to the speed at which the biomass is heated and reacted. Thus, it is desirable to react the biomass as quickly as possible. This inference is supported by Figure 15 which shows CH_4 evolution as a function of time during fast pyrolysis for differing concentrations of CaO in the loaded sample.

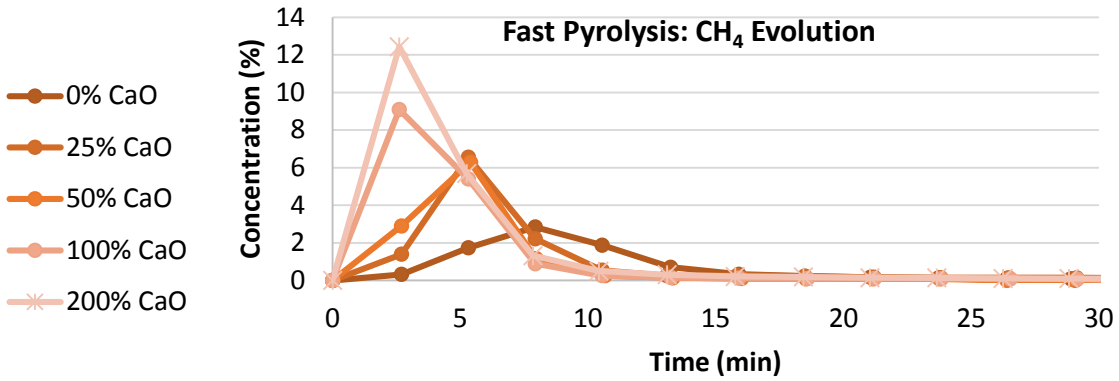

Figure 15: a plot of CH4 evolution as a function time in the reactor outlet gases during fast pyrolysis for varying CaO loadings..

The peak concentration for CH_4 increases with increasing CaO concentration, indicating that catalytic activities are, in fact, taking place. Interestingly, the time until peak concentration decreases with increasing CaO concentration. We can see a similar effect for the production of H_2 during fast pyrolysis for varying CaO concentrations in Figure 16.

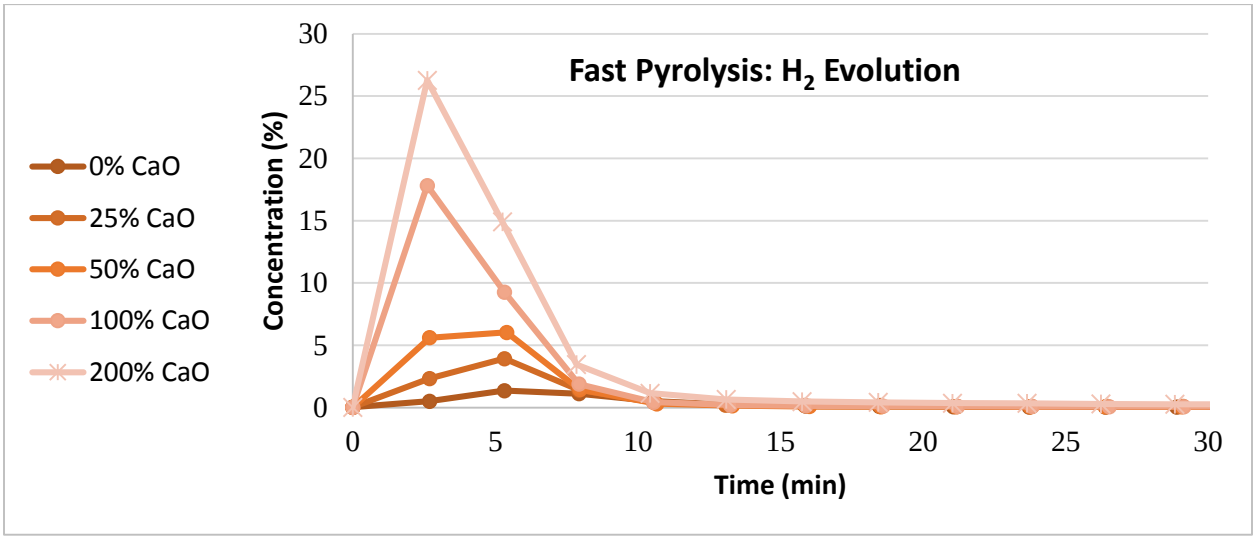

Figure 16: evolution of H_2 during fast pyrolysis for varying CaO loadings.

Again, it is observed that faster evolutions correspond to more generation of fuel gases. Thus, it was of interest to make a statistical model relating the evolution times of the gases out of the reactor as a function

of the CaO concentration; the time until peak concentration of gases was plotted against CaO concentration and a statistical model was developed. These results are summarized in the JMP output in Figure 17.

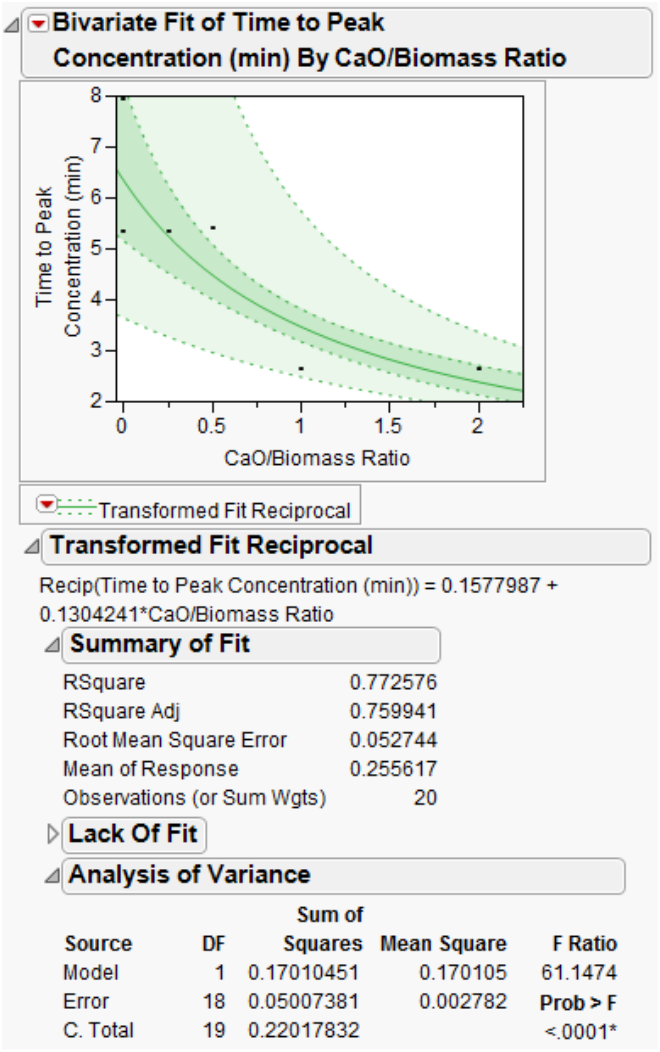

Figure 17: model and statistical analysis on the fit of an inverse relation between time to peak evolution and CaO loading.

From the statistical analysis, we obtain that the inverse model explained the greatest amount of variability in the response variable that was also statistically significant as determined by the ANOVA test. While the lack of fit test indicates that the given model may not be accurate (p-value > alpha), this is likely due to the poor time resolution of the GC sampling times. Based on these results, it is likely that the true time that it takes to decompose the biomass decreases with increasing CaO concentration. As presented in the discussion of Figure 14, it could be predicted that the amount of gases evolved during pyrolysis will increase

corresponding to the reduced required residence time within the reactor since we have already argued that the speed of the decomposition of biomass directly relates to the amount of decomposition that occurs.

The total amount of gas evolved was approximated for the construction of statistical models relating the gas evolved to the concentration of CaO in contact with the biomass loaded.

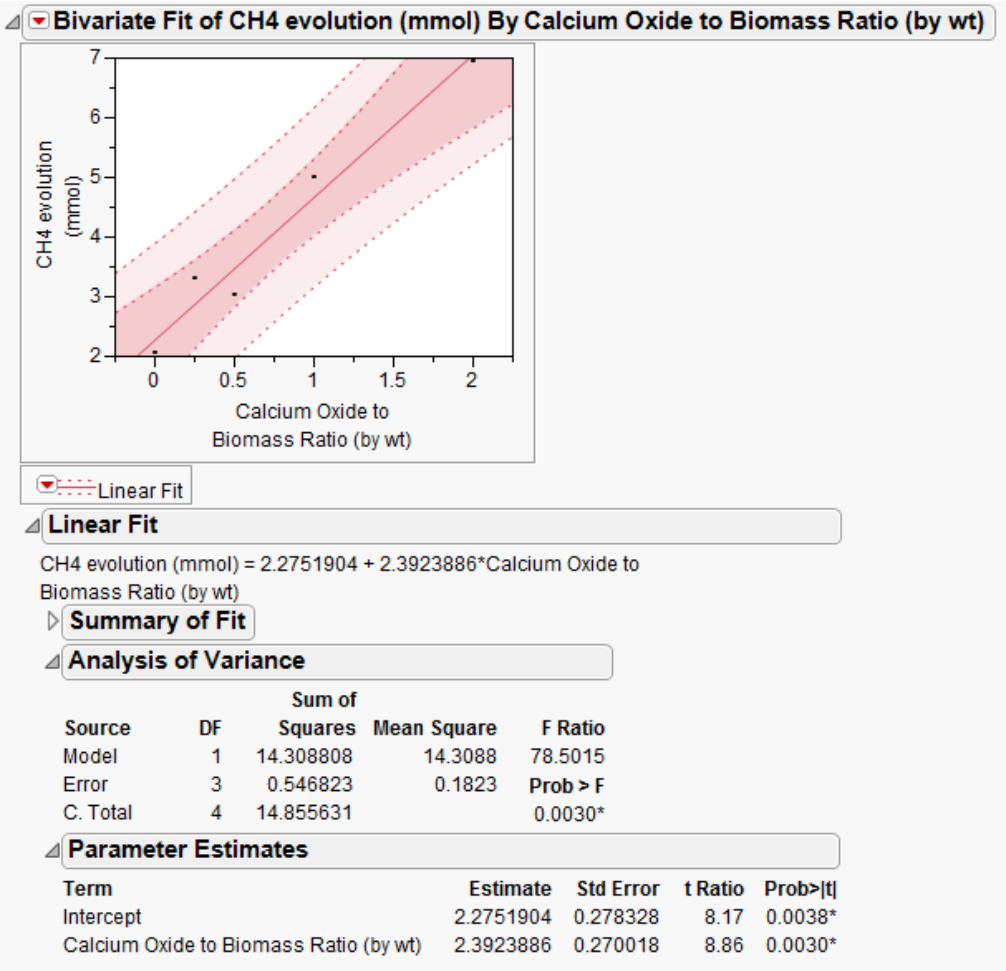

Figure 18: statistical analysis and model of a linear fit to the evolution of CH_4 during pyrolysis as a function of CaO loading.

The analysis reinforces the catalytic capabilities for the decomposition of the biomass to CH_4 and other light volatiles. We can see this further in Figure 19, which shows total H_2 evolution as a function of CaO concentration.

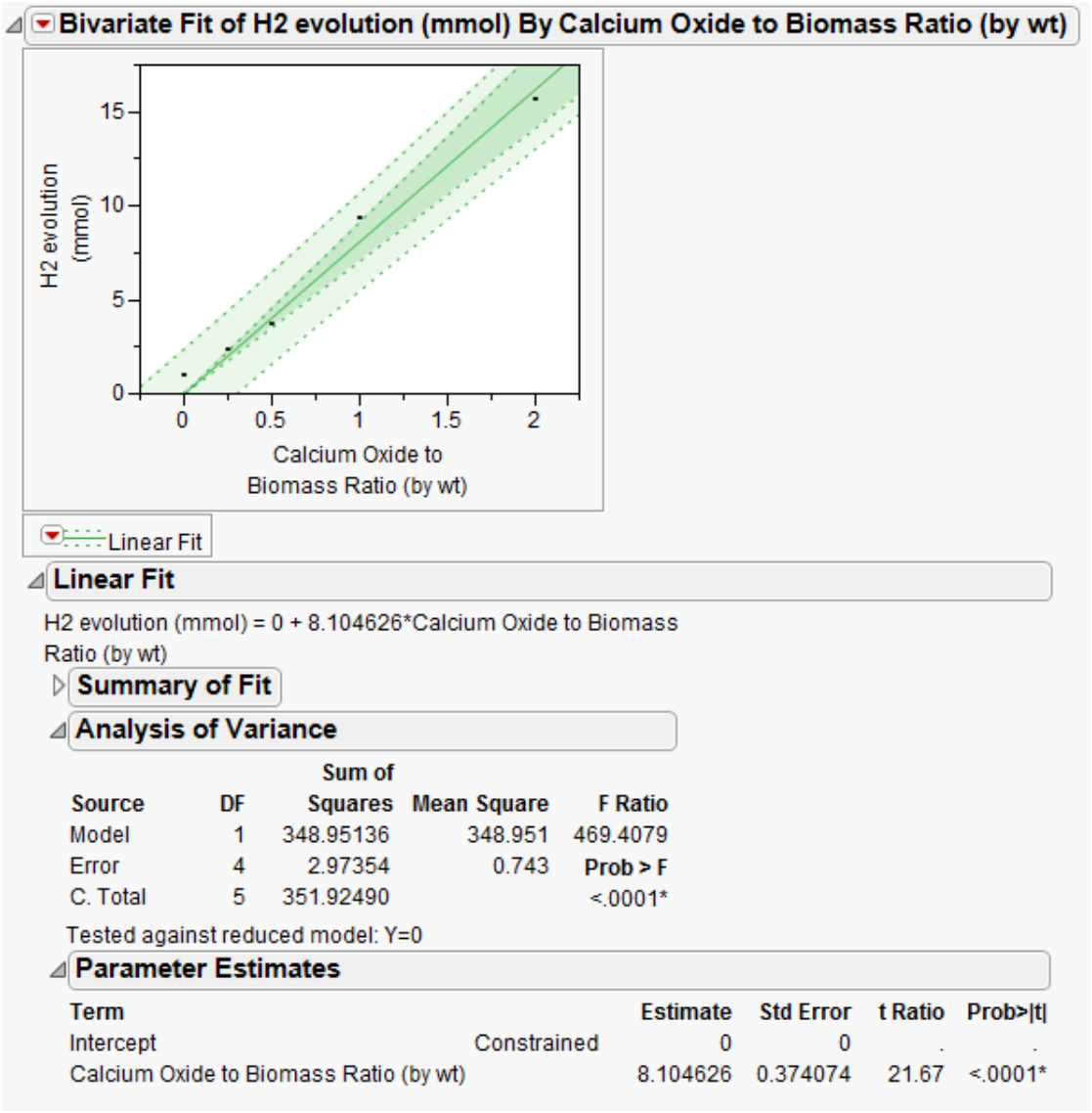

Figure 19: statistical analysis and model of a linear fit to the evolution of H_2 during pyrolysis as a function of CaO loading.

For the analysis in Figure 19, it was determined that while the overall linear model provides a much better explanation than the null model, the y-intercept term was not considered statistically significant. Thus, that parameter was removed from the fit equation. Again, with 95% confidence, we can see monotonically increasing evolution of gases and other compounds with a constant amount of biomass supplied to the reactor. We would like to have said something about the amount of CO and CO_2 evolved, but we can see from the analyses in Figures 20 and 21, respectively, that there is no statistically significant model which can accurately describe the behavior of the amounts evolved.

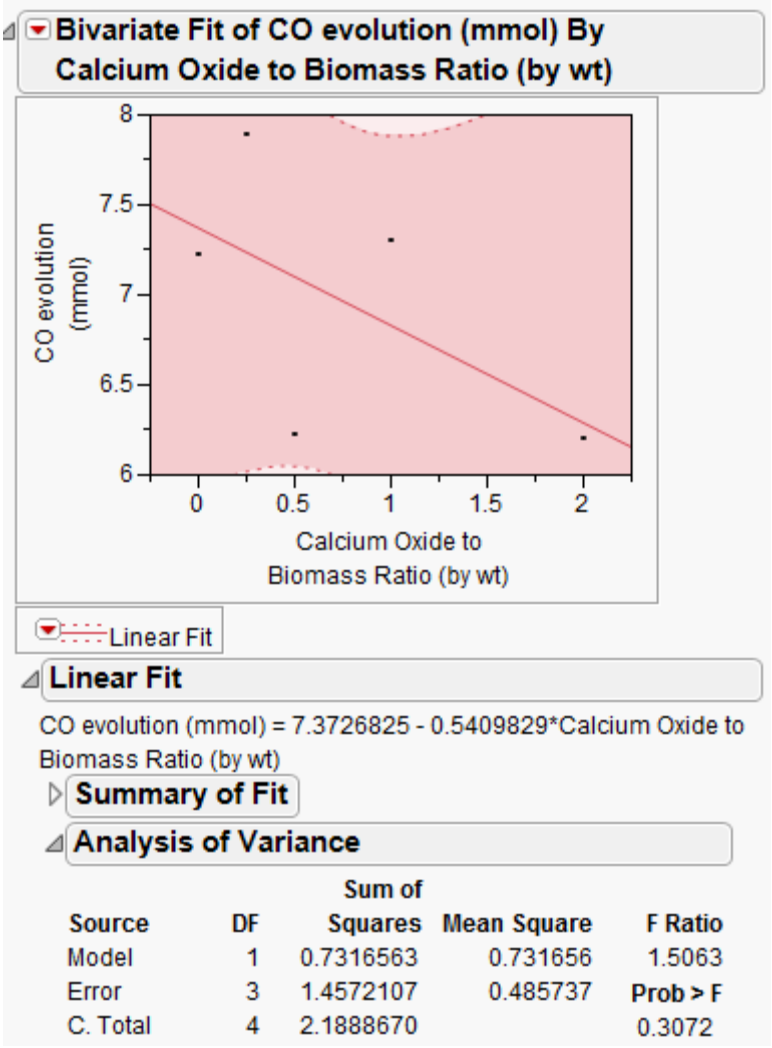

Figure 20: statistical analysis and model of a linear fit to the evolution of CO during pyrolysis as a function of CaO loading.

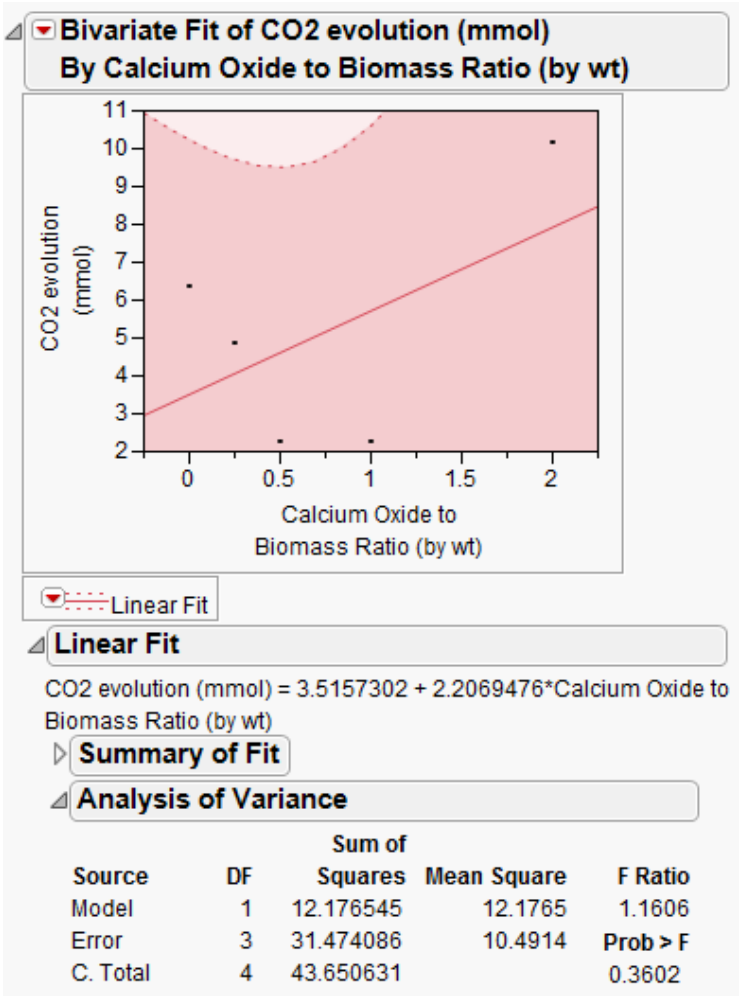

Source	DF	Sum of Squares	Mean Square	F Ratio
Model	1	12.176545	12.1765	1.1606
Error	3	31.474086	10.4914	Prob > F
C. Total	4	43.650631		0.3602

Figure 21: statistical analysis and model of a linear fit to the evolution of CO during pyrolysis as a function of CaO loading.

We fail to obtain any sort of model which could explain the observed variability better than the null model. However, an interesting trend is observed in the data for CO_2 evolution: the total amount of CO_2 seems to monotonically decrease with increasing CaO concentration, up until 200wt% concentration, where the CO_2 unexpectedly spikes; this can be seen clearly in Figure 22.

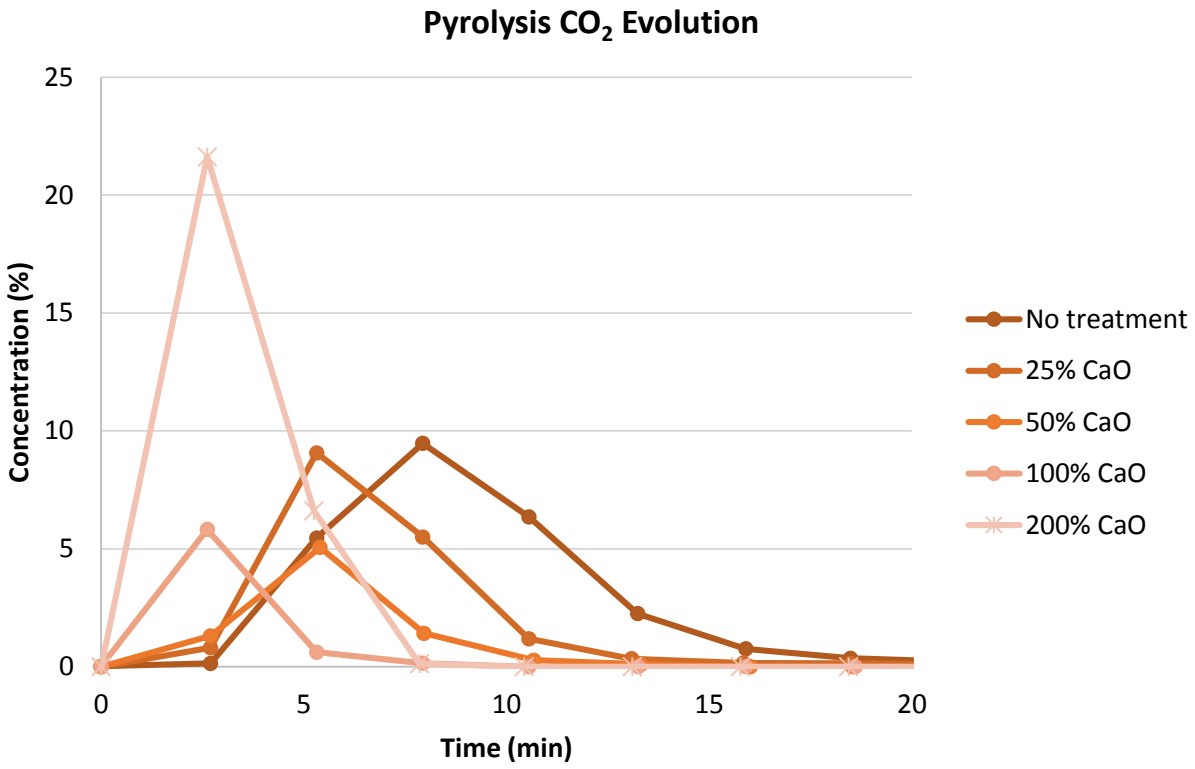

Figure 22: CO_2 concentration in the exit gases from the reactor during pyrolysis plotted against time at varying CaO wt%.

This is an unexpected result; the CO_2 concentration is expected to decrease since CaO is a CO_2 capture agent. Thus, we can observe that there is and unexplained decrease in the amount of CO_2 capture occurring inside the reactor occurring at a sufficiently high wt% of CaO. It could imply that the catalytic effects of CaO are much more important and faster on the reactor residence timescale than the CO_2 capture is.

Another factor of interest was the amount of bio-oil produced during pyrolysis; thus, the amounts of bio-oil that were condensed out of the reactor effluent were collected after every test, weighted, and plotted against the CaO concentration in the sample loading. The resulting graph and statistical analysis may be found in Figure 23.

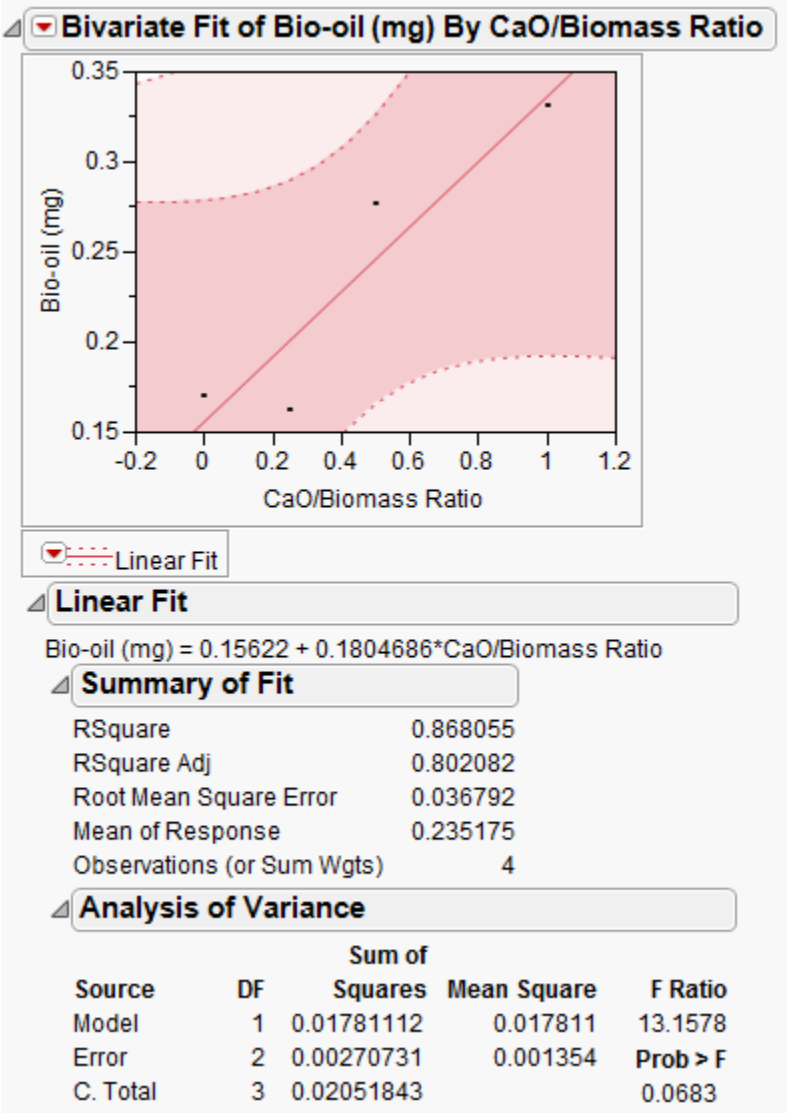

Figure 23: statistical analysis and model of a linear fit to the evolution of bio-oil during pyrolysis as a function of CaO loading.

The 200wt% concentration was omitted due to the observed reaction behavior shift at that concentration; a relation corresponding to the normal behavior of increasing concentration of CaO was desired. While we fail to reject the null model in favor of the linear one, a high R^2 value seems to suggest that this model would explain much of the observed variability. This implies that statistical result in Figure 23 may be a Type II error; we would have likely formed an explanatory relationship with additional points. At the 200wt% concentration of CaO, no bio-oil condensation was observed. This observation is against the observed trend; however, this could help to explain the higher-than-expected CO_2 concentration observed

in the reactor effluent. This could imply that at sufficiently high concentrations of CaO, we see the CaO breaking down the light tars evolved from the decomposition of the biomass.

Gasification Results

For gasification of the biomass/CaO mixture, we see similar results to that of pyrolysis for the evolution of H_2 and CH_4. Total H_2 and CH_4 evolution amounts were plotted against the concentration of CaO in the feed in Figures 24 and 25, respectively.

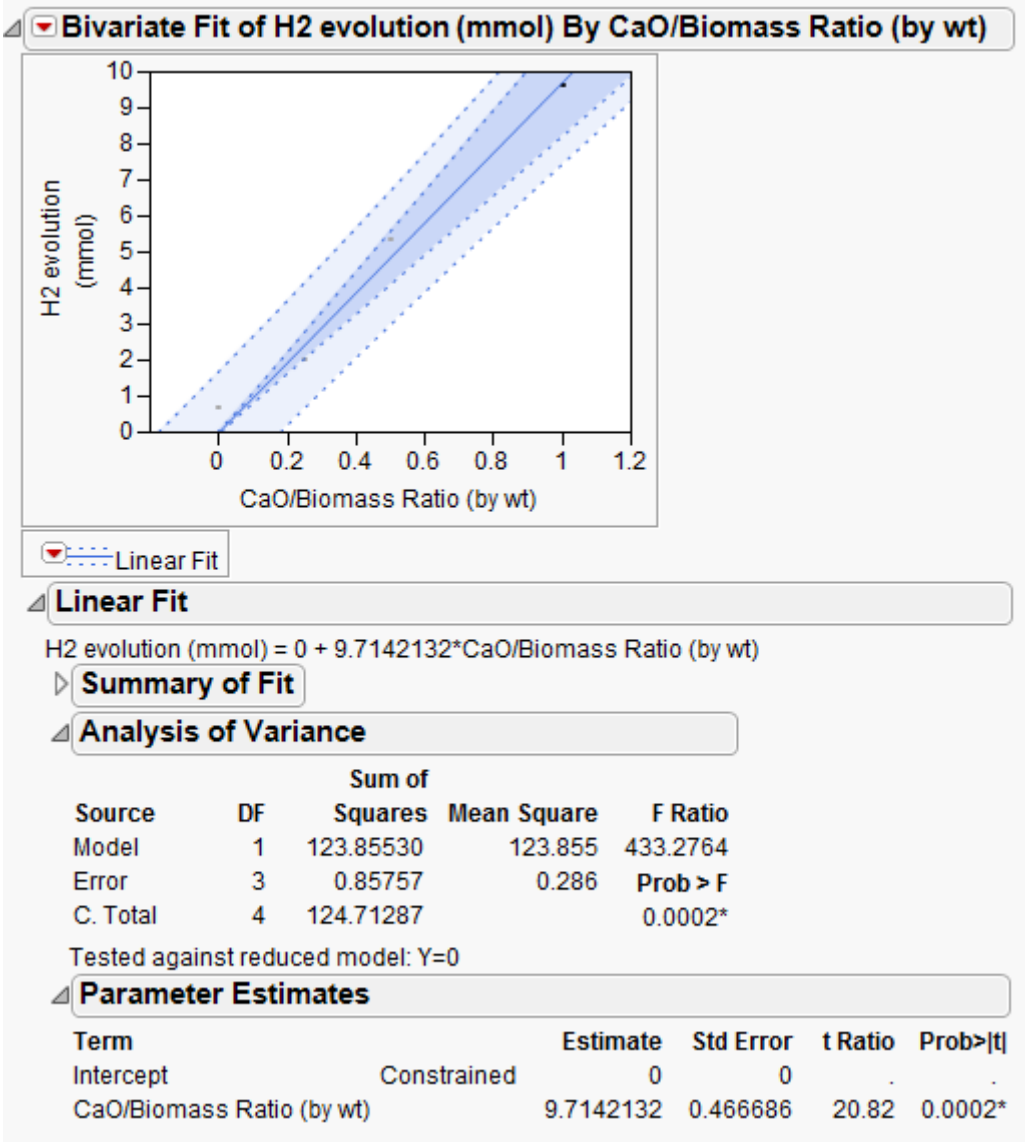

Figure 24: statistical analysis and model of a linear fit to the evolution of H_2 during gasification as a function of CaO loading.

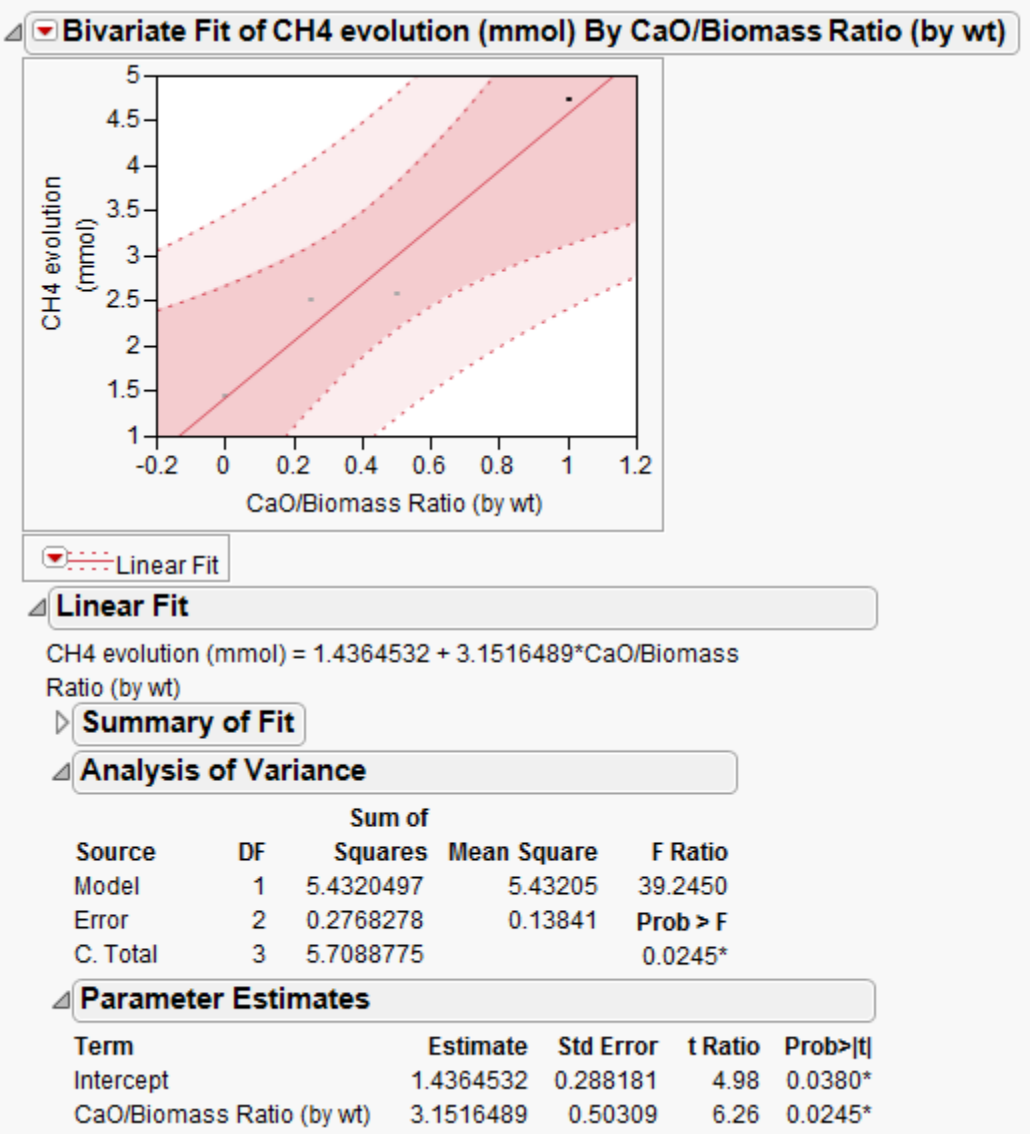

Figure 25: statistical analysis and model of a linear fit to the evolution of CH_4 during gasification as a function of CaO loading.

We can observe monotonically increasing amounts of the fuel gases evolved as a function of CaO concentration. Overall, this is promising for implementation of a calcium looping system for both the pyrolysis and gasification of biomass.

We cannot prove any relation or model for the evolution of CO or CO_2 during gasification, but for similar reason as we could not prove one for the evolution of CO_2 during pyrolysis. Looking at Figure 26, we see that CO and CO_2 concentrations in the exit gases increase sharply at 100% CaO during gasification.

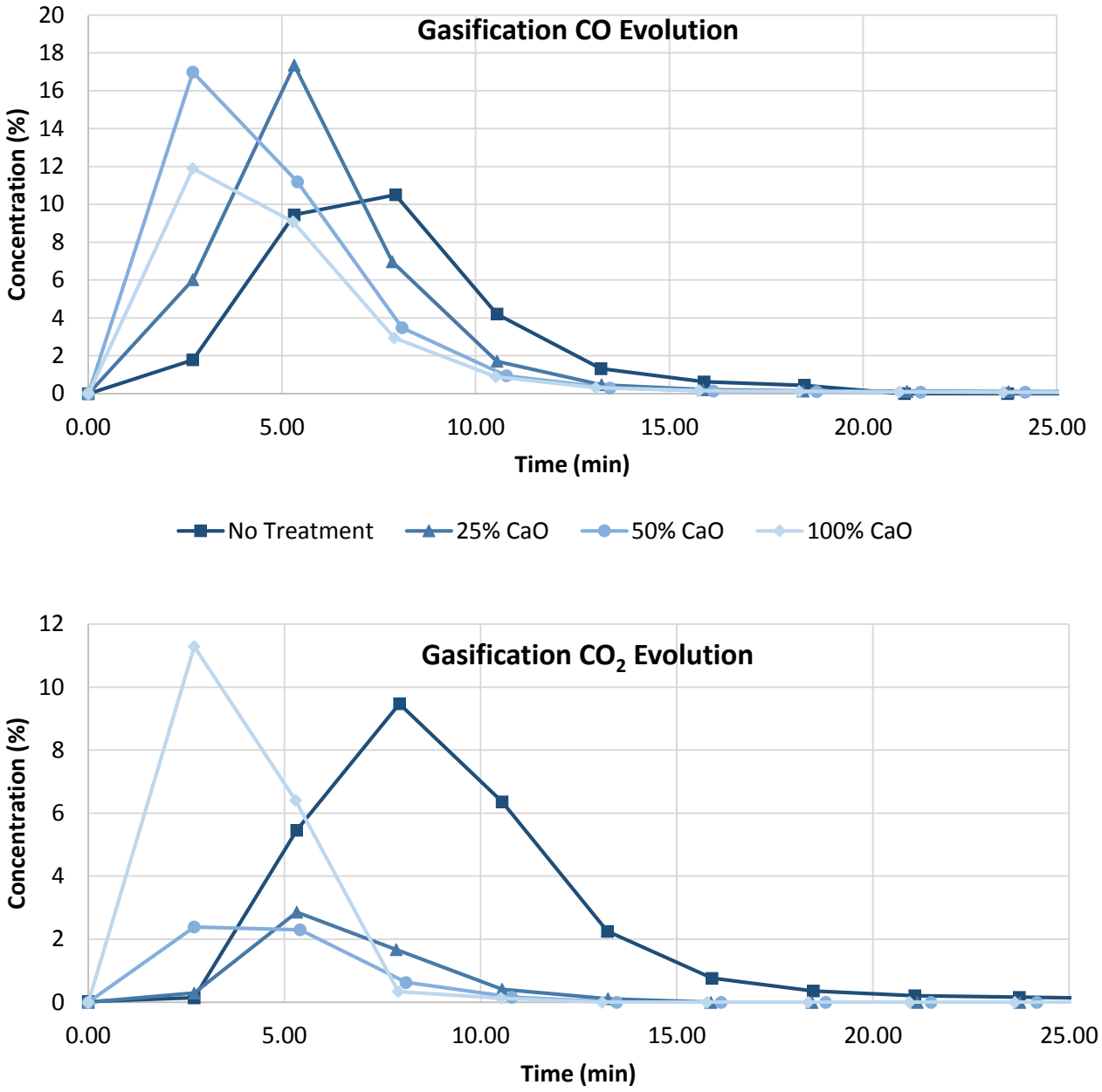

Figure 26: CO and CO2 concentration in the reactor exit gases as a function of time for varying CaO loadings.

We see the same type of reactor dynamic shift that we saw for 200wt% CaO during pyrolysis, but now at 100 wt% for gasification. This effectively indicates that the immediate presence of the CaO catalyst can effectively increase the combustion and conversion of the biomass fuels, especially at very high concentrations.

Gasification with $Ca(OH)_2$ as the Source of Steam

In terms of proof-of-concept for the implementation of the calcium looping system, it would be advantageous to show that $Ca(OH)_2$ could be used as the source of oxidizing agent during gasification. To this end, the gasification and pyrolysis of solid biomass mixture with 50% CaO. Thus, in Figure 27 we see how the supply of oxidizing agent via CaO compares against pure pyrolysis and true gasification at 30% steam concentration.

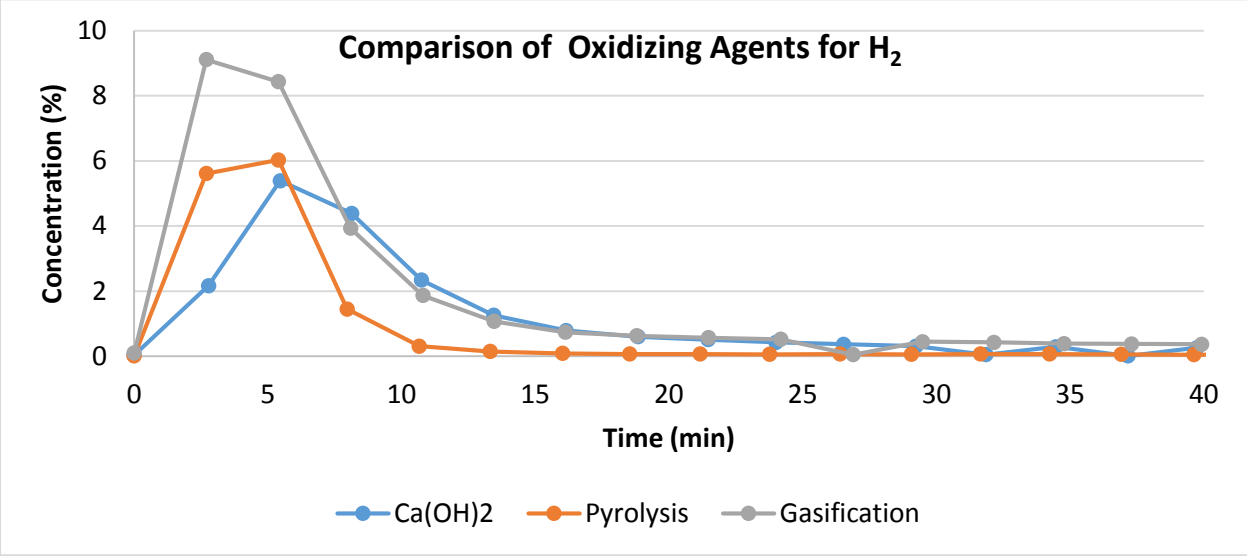

Figure 27: concentration of H2 plotted against time for different methods of oxidation at 50wt% CaO.

From the graph of the production of H_2, it is evident that 50wt% CaO is not effective enough for the gasification. However, when we look at Figure 28 to see the concentration of CO in the exit gas stream for the different oxidation methods, we see information that may help develop an explanation as to why the amount of H_2 evolved does not increase with $Ca(OH)_2$ loading.

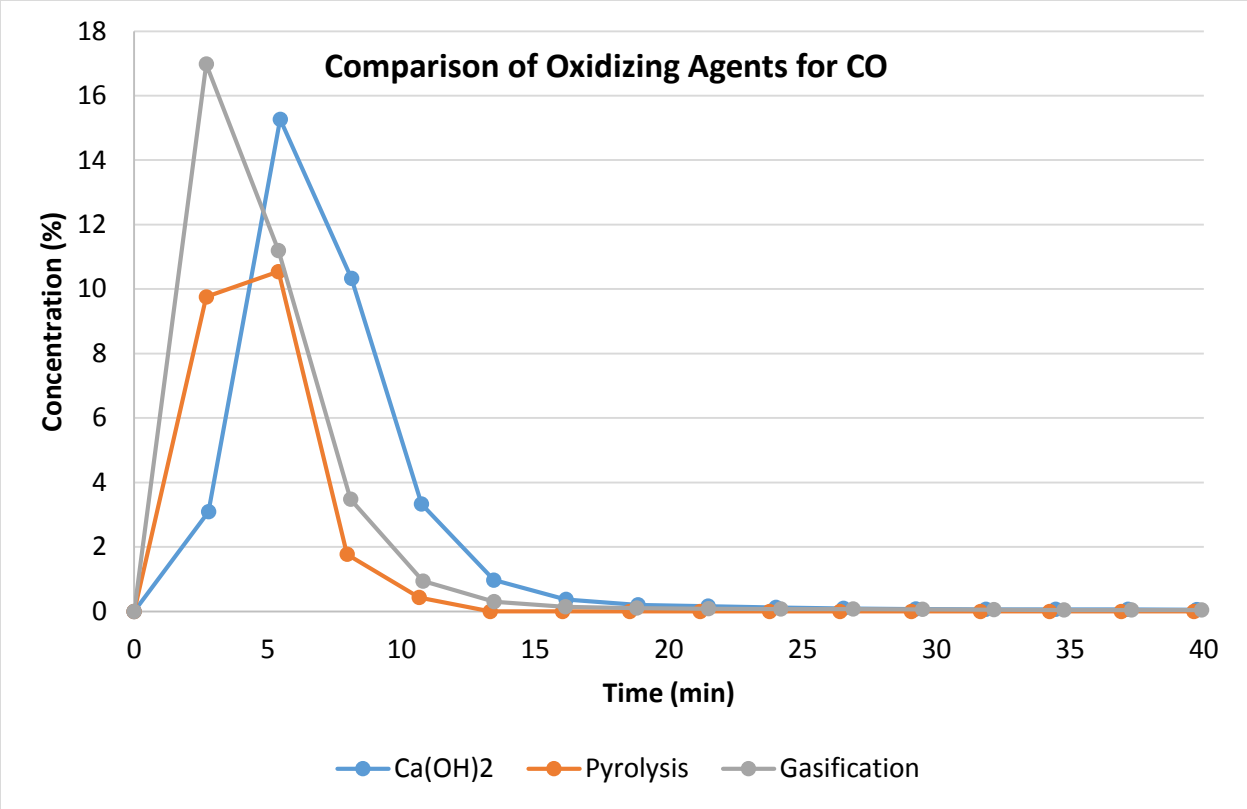

Figure 28: concentration of CO plotted against time for different methods of oxidation at 50wt% CaO.

It can be observed that there is generation of CO for $Ca(OH)_2$ as the source of steam comparable to true gasification, indicating that partial oxidation is occurring. Thus, it is likely that the ineffectiveness of the $Ca(OH)_2$ as the source of the oxidizing agent is likely due to the extreme shortage of the amount of oxidizing agent being fed to the reactor as compared to conventional gasification. The amount of CaO loading is the same for all types of oxidation, so the catalytic effects should be similar. One may ask why the H_2 concentration does not increase when clearly partial oxidation is occurring. One possible explanation may be that the initial evolution of CO as a result of the steam oxidation actually captures the hydrogens in the biomass complex by forming oxygenated functional groups in the place of the CO groups, and that additional oxidation is required in order to fully decompose those functional groups and produce hydrogen.

IV. CONCLUSIONS & RECOMMENDATIONS

From the results gathered in this study, several conclusions can be made. First, increasing CaO concentration relative to biomass increases the amount of gases evolved per gram of biomass fed for both pyrolysis and gasification; in other words, the overall yield of fuel from biomass increases. There is likely some theoretical concentration where each particle of biomass is completely surrounded by CaO, at which point feeding additional CaO would not be beneficial for increased conversion; it would be of interest to study this upper theoretical limit. However, it is much more likely that the process will be limited by the amount of biomass that would needed to be processed over a certain timescale, at which point the energetic requirements for the transportation/circulation and concurrent regeneration of proportionally high quantities of CaO would have to be considered. Second, it is theorized that the catalytic properties of the CaO is much faster and are much more important to the evolution of fuel gases than the chemisorbing capture capabilities of CaO for gases such as $CaCO_3$. At sufficiently high concentrations of CaO we saw that the level of overall conversion of biomass increased significantly, and that even the light tars that are typically evolved from the process were catalytically decomposed in the vapor phase. Experiments on the decomposition of these light tars in the gas phase using a CaO bed should be done in a more controlled manner to determine if this theory is valid. Lastly, $Ca(OH)_2$ would likely be effective as a gasification agent only if it were present in large excess quantities relative to the amount of biomass fed correspondingly. It is likely that only at very high concentrations of $Ca(OH)_2$ that the evolution of gases will be similar to that of true gasification with a similar CaO loading.

In terms of future work, higher concentrations of $Ca(OH)_2$ should be tested in order to verify its capabilities as source of the gasification agent. Additionally, we should explore the higher (200%+) concentrations of CaO on the gasification and pyrolysis of biomass. Further, and perhaps most importantly, we should study the level of decomposition of the char in the calciner. From there, the relationship between the amount of purge from the process and the circulation of char within the looping mechanism can be estimated.

Circulating large amounts of char would have an additional energetic requirement in terms of the capital cost of equipment, operating costs, and would likely interfere with catalytic capabilities of the CaO. Ideally, all of the char would be combusted in the calciner in order to reduce the energy needed for calcination (an endothermic reaction). Further, regeneration testing should be carried out on CaO to determine its robustness against deactivation in a catalytic looping mechanism. Lastly, extensive modeling of the overall process will be required in order to determine its suitability for scale-up.

Overall, the proposed CaO looping process shows some promise on a proof-of-concept scale. However, much more work will need to be done in order to determine its suitability as an industrial process for the conversion of biomass to fuels.

REFERENCES

Blamey, J., et al. (2010). "The calcium looping cycle for large-scale CO2 capture." Progress in Energy and Combustion Science **36**(2): 260-279.

Borgwardt, R. H. (1989). "Calcium oxide sintering in atmospheres containing water and carbon dioxide." Industrial & Engineering Chemistry Research **28**(4): 493-500.

Fan, L., et al. (2008). "Utilization of chemical looping strategy in coal gasification processes." Particuology **6**(3): 131-142.

Florin, N. H. and A. T. Harris (2008). "Enhanced hydrogen production from biomass with in situ carbon dioxide capture using calcium oxide sorbents." Chemical Engineering Science **63**(2): 287-316.

García, X. A., et al. (1999). "Steam gasification of tars using a CaO catalyst." Fuel Processing Technology **58**(2–3): 83-102.

Han, J. and H. Kim (2008). "The reduction and control technology of tar during biomass gasification/pyrolysis: An overview." Renewable and Sustainable Energy Reviews **12**(2): 397-416.

Lin, S.-Y., et al. (2001). "Hydrogen Production from Hydrocarbon by Integration of Water−Carbon Reaction and Carbon Dioxide Removal (HyPr−RING Method)." Energy & Fuels **15**(2): 339-343.

Ramkumar, S. and L.-S. Fan (2010). "Calcium Looping Process (CLP) for Enhanced Noncatalytic Hydrogen Production with Integrated Carbon Dioxide Capture." Energy & Fuels **24**(8): 4408-4418.

Ramkumar, S. and L.-S. Fan (2010). "Thermodynamic and Experimental Analyses of the Three-Stage Calcium Looping Process." Industrial & Engineering Chemistry Research **49**(16): 7563-7573.

Seshadri, K. S. and A. Shamsi (1998). "Effects of Temperature, Pressure, and Carrier Gas on the Cracking of Coal Tar over a Char−Dolomite Mixture and Calcined Dolomite in a Fixed-Bed Reactor." Industrial & Engineering Chemistry Research **37**(10): 3830-3837.

Taralas, G., et al. (1991). "Thermal and catalytic cracking of n-Heptane in presence of CaO, MgO and Calcined Dolomites." The Canadian Journal of Chemical Engineering **69**(6): 1413-1419.

Wang, W., et al. (2010). "Subpilot Demonstration of the Carbonation−Calcination Reaction (CCR) Process: High-Temperature CO2 and Sulfur Capture from Coal-Fired Power Plants." Industrial & Engineering Chemistry Research **49**(11): 5094-5101.